Caco-2 cell-based electrochemical biosensor for evaluating the antioxidant capacity of *Asp-Leu-Glu-Glu* isolated from dry-cured Xuanwei ham

Lujuan Xing, Qingfeng Ge, Donglei Jiang, Xiaoge Gao, Rui Liu, Songmin Cao, Xinbo Zhuang, Guanghong Zhou, Wangang Zhang

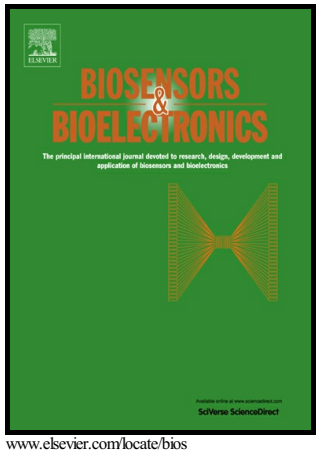

www.elsevier.com/locate/bios

PII: S0956-5663(18)30027-7
DOI: https://doi.org/10.1016/j.bios.2018.01.020
Reference: BIOS10213

To appear in: *Biosensors and Bioelectronic*

Received date: 6 November 2017
Revised date: 8 January 2018
Accepted date: 9 January 2018

Cite this article as: Lujuan Xing, Qingfeng Ge, Donglei Jiang, Xiaoge Gao, Rui Liu, Songmin Cao, Xinbo Zhuang, Guanghong Zhou and Wangang Zhang, Caco-2 cell-based electrochemical biosensor for evaluating the antioxidant capacity of *Asp-Leu-Glu-Glu* isolated from dry-cured Xuanwei ham, *Biosensors and Bioelectronic,* https://doi.org/10.1016/j.bios.2018.01.020

Caco-2 cell-based electrochemical biosensor for evaluating the antioxidant capacity of *Asp-Leu-Glu-Glu* isolated from dry-cured Xuanwei ham

Lujuan Xing[a], Qingfeng Ge[a,b], Donglei Jiang[b], Xiaoge Gao[a], Rui Liu[a], Songmin Cao[a], Xinbo Zhuang[a], Guanghong Zhou[a], Wangang Zhang[a,*]

[a] *Key Laboratory of Meat Processing and Quality Control, MOE; Key Laboratory of Meat Processing, MOA; Jiangsu Synergetic Innovation Center of Meat Processing and Quality Control; Nanjing Agricultural University; Nanjing, 210095, P.R. China*

[b] *School of Food Science and Technology, Yangzhou University, Industrial Engineering Center for Huaiyang Cuisine of Jiangsu Province,Yangzhou, Jiangsu 225127, P.R. China*

*Corresponding author: Wangang Zhang
E-mail addresses: wangang.zhang@njau.edu.cn

Abstract: A cell-based electrochemical biosensor was developed to determine the antioxidant activity of Asp-Leu-Glu-Glu (DLEE) isolated from dry-cured Chinese Xuanwei ham. A platinized gold electrode (Pt NPs/GE) covered with silver nanowires (Ag NWs) was fabricated to detect H_2O_2 using redox signaling via cyclic voltammetry (CV), differential pulse voltammetry (DPV), and electrochemical impedance spectroscopy (EIS). Under optimal condition, the detection limit of the modified electrode was 0.12 μM with a linear relationship from 0.2~2 μM, which showed relatively outstanding catalytic effects towards the reduction of H_2O_2. Furthermore, the generation of reactive oxygen species (ROS) in the cell can be used to indirectly assess changes in intercellular oxidative stress by detecting variations in electrochemical signals. A 3D cell culture of alginate/graphene oxide (NaAlg/GO) was used to encapsulate and immobilize Caco-2 cells. Based on ROS generation and electrochemical results, we found that DLEE could effectively reduce oxidative stress level in Caco-2 cells under external stimulation. DLEE showed high antioxidant activity with a relative antioxidant capacity (RAC) rate of 88.17% at 1.5 mg/mL. Finally, an efficient electrochemical biosensor was established using the active 3D Caco-2 cell platform. This system is sensitive and simple to operate with the property to evaluate the antioxidant activity of peptides by the detection of H_2O_2 in cell membrane. In summary, this work describes a new method for assessing antioxidant capacity of peptide DLEE using cell-based electrochemical signaling with a rapid screening pattern.

Keyword: Caco-2 cells; *Asp-Leu-Glu-Glu*; Hydrogen peroxide; Antioxidant activity; Electrochemical assay

1. Introduction

Bioactive peptides are functional molecules containing 4~20 amino acids that have positive effects on the functioning and internal environment of human body (Samaraweera et al., 2011). In recent years, antioxidant peptides have attracted much attention due to their acting ability to prevent oxidative stress associated with cell and DNA damage. Research has shown that antioxidant peptides can inhibit the generation of reactive oxygen species (ROS) by scavenging free radicals, preventing the transition of pro-oxidative metal chelation and reducing hydroperoxide formation (Gao et al., 2012). Meat, poultry, fish and fermented animal products are the primary sources of purifying antioxidant peptides (Liu et al., 2016; Sarmadi and Ismail, 2010).

In previous studies on the purification and selection of antioxidant peptides, chemical assays were the main methods to determine antioxidant activity, including free radical scavenging, metal chelation, and stimulating active molecules *in vitro* chemical systems (Sila and Bougatef, 2016). Compared to chemical assays, cell-based antioxidant effects would be more sensitive for determining antioxidant function. Antioxidant peptides from the hydrolysis of the fish skin caused a decrease in ROS generation in human breast adenocarcinoma cells by fluorescence detection (Sudhakar and Nazeer, 2015). Reports have confirmed that antioxidant peptides can protect cell membranes based on the scavenging activity of ROS (Pillai et al., 2006; Torres-Fuentes et al., 2015). It is widely known that ROS are generated during all processes of cell growth, reproduction, differentiation, development, aging, and apoptosis, as well as in various pathological contexts. H_2O_2 is the main composition of ROS and the measurement of the H_2O_2 level is vital for assessing oxidative stress in living cells (Bai et al., 2016). Chakraborty and Raj (2009) firstly used electrochemical strategies to assess the antioxidant capacities of bacterial compositions with high sensitivity and

rapid detection. Recent reports have utilized enzymatic and non-enzymatic electrochemical biosensors to measure H_2O_2 in living cells so as to evaluate oxidative stress levels (Feng et al., 2013; Prakash et al., 2015). In particular, cyclic voltammetry (CV) and differential pulse voltammetry (DPV) are extensively used for real-time screening with dynamic kinetic characteristics and high resolution to identify redox signing with electrical patterns (Nandini et al., 2017; Prakash et al., 2015). Some reports have focused on modifying electrodes to increase the sensitivity and the stability of the biosensors. However, no published studies have ever utilized the sensitive electrodes to analyze the protective effects of natural antioxidant peptides in living cells. Therefore, we attempted to adopt an electrochemical biosensor for measuring cell-based oxidative stress as a novel method for evaluating the antioxidant activity of functional peptides.

The Caco-2 cell culture system is commonly used to evaluate the functional activity of medicines and other bioactive compounds in the previous assays (Artursson et al., 2012; Sun et al., 2006). Fish skin gelatin, eggshell membrane peptides and squid antioxidant peptides have been demonstrated to improve cellular enzyme activity and exert cytoprotective effects in cells (Shi et al., 2014a; Sila and Bougatef, 2016; Sudhakar and Nazeer, 2015). Eggshell membrane peptides can regulate the synthesis of glutathione to protect against oxidative damage in Caco-2 cells (Shi et al., 2014b). Stable stimulation of H_2O_2 causes Caco-2 cells to generate more ROS, and the fluorescence intensity of cells could be reduced by cultivation with antioxidant peptides from corn gluten meal (Wang et al., 2016). Therefore, the wide investigation on Caco-2 cells supplied the precondition for the fabrication of electrochemical biosensors.

Platinum nanoparticles (Pt NPs) have been widely used to increase electrocatalytic current and enhance electrode sensitivity for detecting H_2O_2 (Liu et al., 2015; Zhou and Ma, 2017). Ag NWs also show excellent catalytic activity for H_2O_2 reduction and can also decrease interfering signals from other molecules including ascorbic acid and uric acid (Chen et al., 2010). To fabricate a sensitive and rapid electrochemical biosensor, a bare gold electrode was electroplated with Pt NPs as well as Ag NWs on the surface. Graphene oxide (GO) was an efficient substratum to promote the adhesion and proliferation of cells, which could also promote the electrical conductivity as well as the biocompatibility so as to provide a suitable environment for the development of cells (Kim et al., 2013). With the purpose of keeping the cell activity and also increasing the adhesion of cell suspension, GO was added in the cell suspension for the fabrication of 3D structure to buffer cells from environmental influences (Lei et al., 2014).

In the current study, a novel non-enzymatic electrochemical sensor was fabricated based on a modified Pt NPs/Ag NWs/GE which showed relatively high electrocatalytic efficiency for detecting H_2O_2 level in the cells. A 3D culture system was used to enhance the activity and the integrity of cells on the surface of electrodes and maintain stability during electron transfer. The antioxidant effects and redox profile of peptide Asp-Leu-Glu-Glu (DLEE) were evaluated under oxidative stress conditions. The redox signaling pattern was further investigated using CV, DPV, and EIS. In addition, ROS generation, antioxidant enzyme activity and apoptosis were also performed to compare the biochemical and electrochemical sensor results.

2. Experiments

2.1. Materials

Silver nanowires and graphene oxide were purchased from Xianfeng Nanomaterials Technology Co. Ltd. (Nanjing, China). Caco-2 cells, DMEM, phosphate buffer (1×, pH 7.4), fetal bovine serum and a cell apoptosis kit were obtained from Kaigen BioCo. (Nanning, China). Sodium alginate (NaAlg), calcium oxide, calcium chloride ($CaCl_2$) and hydrogen peroxide (H_2O_2, 30%) were purchased from Sigma-Aldrich Inc. (St. Louis, MO, USA). The kit for measuring antioxidant enzyme activity was obtained from Jiancheng (Nanning, China). All other chemicals were analytical grade and purchased from Solarbio Life Science (Beijing, China).

2.2. Electrochemical working system

A CHI660E electrochemical workstation with a three-electrode system was purchased from Chenhua Technology Co. Ltd. (Shanghai, China). A counter electrode of Pt wires (1 mm diameter), a reference electrode of Ag/AgCl (in KCl) and a working electrode for the cell-based sensor comprised the electrochemical apparatus. The structure of Ag NWs and cell morphologies were characterized using Scanning Electron Microscopy (Tecnai 12, Philips, Netherlands). The X-ray diffraction (XRD) pattern of silver nanowires was recorded by Rigaku D/max-ra with Cu Kα radiation (λ=1.5418Å) by the diffractometer (2500 vl, Rigaku, Japan). Caco-2 cells were cultured in a CO_2 incubator (Thermo Fisher Scientific Inc., Rockford, Illinois, USA).

2.3. Fabrication of the cell-based sensor

Caco-2 human intestinal cells were cultured in DMEM with 10% FBS and 1% penicillin-streptomycin at 37°C in 5% CO_2. Cells from passages 20~50 were used for all experiments with a generation time of 5~6 d. During cultivation, the medium was replaced every 2 d.

A bare gold electrode was polished by Al_2O_3 (first with 0.3 mm and then with 0.05 mm) for 5 min and ultrasonically washed in distilled water. The bare gold electrode was

electrochemically pretreated in a 10 mM H_2PtCl_6 solution under a voltage of -0.2 V with a 100 mV/s scanning rate for 300 s (Bai et al., 2016). The initial concentration of Ag NWs was 20 mg/mL which was diluted to a gradient by distilled water. Subsequently, 5 μL Ag NWs were deposited onto the electrode and dried for 20 min until being stable. CV and DPV were used to determine the characteristics of the modified electrode.

To determine the sensitivity of modified electrode, H_2O_2 was measured by exogenous addition into the modified Pt NPs/Ag NWs/GE with a gradient concentration from 0.2 μM to 1000 μM. A magnetic bead inside the working solution was used for blending. Depending on the detection of redox signaling, the cell-based biosensor was subsequently prepared. In order to stick the Caco-2 cells onto the modified electrode as tight as possible, hydrogels were prepared using sodium alginate (NaAlg) to maintain cell activity and GO to support the 3D gel structure (Jiang et al., 2017). To encapsulate the cells inside the hydrogel, a logarithmic batch of Caco-2 cells were washed and resuspended in DMEM. Then, 1 mL cell suspension was added to 1 mL NaAlg/GO hydrogels following with incubation in 37 ℃ incubators for 5 min. Finally, 5 μL of cell hydrogels were dropped onto the modified electrode following with immobilization in 100 mM $CaCl_2$ dissolved in DMEM for 3 min. After fabrication, the cell-based biosensor was investigated carefully. Finally, CV, DPV and EIS signals were monitored using the CHI660E electrochemical workstation. A potential range of -0.2 V to +0.6 V was scanned in CV with a rate of 100 mV/ s whereas the potential range of DPV was -0.4 V to +0.6 V with 0.05 V for a pulse amplitude, 0.05 s for pulse width and 0.2 s for pulse period. The operation was performed at 25 ℃ to maintain the proper conditions for the CHI660E electrochemical workstation.

2.4. Caco-2 cell culture and pretreatment of oxidative stress

The oxidative stress of cells was determined using the methods of Shi et al.(2016) with slight modifications. The Caco-2 cells were incubated at an initial concentration of 2×10^5 cells/mL in 6-well culture plates (Corning Costar, Corning, New York, USA). After cultivation for 5 d, the medium was replaced with Hank's balanced salt solution (HBSS, no calcium and magnesium). Four treatments were as follows: blank group without treatment, oxidative group with H_2O_2 treatment (1 mM) for 2 h; protective group Ⅰ with DLEE pretreatment (0.5 mg/mL, 1.0 mg/mL and 1.5 mg/mL) for 12 h and cultivation in H_2O_2 (1 mM) for another 2 h; protective group Ⅱ with GSH pretreatment (0.5 mg/mL, 1.0 mg/mL and 1.5 mg/mL) for 12 h and then placed in oxidative stress with H_2O_2 similar to group Ⅰ. Finally, the four groups of cells were collected and suspended in DMEM to detect H_2O_2 level.

To describe the antioxidant capacity more intuitively, relative antioxidant capacity (RAC) was calculated following the equation in Ge et al. (2018):

$$RAC = (I_0\text{-}I_s) / (I_0\text{-}I) \times 100\%$$

where all values are the peak current in DPV analysis. I_0 represents the peak current for H_2O_2 treatment in oxidative group; I_s represents the peak current of the protective group with peptide treatment; and I represents the blank group without any treatment.

2.4.1 Conventional cell-based assays for antioxidant measurements

Following the four groups of treatments, cellular ROS levels were tested by fluorescence detection (Sudhakar and Nazeer, 2015). The cell plate was washed twice with phosphate-buffered saline (PBS) and treated with 2,7-dichlorodihydrofluorescein diacetate (DCFH-DA, 10μM) for 30 min at 37°C. The Caco-2 cells were collected and then washed twice with PBS again. Intracellular ROS signals were observed using Leica SR GSD (DMI 6000 B, Leica, Germany) with a fluorescent light channel. Cells

were then moved to black 96-well plates to detect the fluorescence index using a Multimode Reader (Molecular Devices, California, USA) at an excitation wavelength of 485 nm and an emission wavelength of 535 nm.

2.4.2. Antioxidant enzyme activity

Cell apoptosis was evaluated by flow cytometry using an Annexin V-APC/PI Apoptosis Detection Kit (Kaigen Bio.CO, Nanjing, China). Briefly, Caco-2 cells (5×10^6 cells/mL) were incubated with DLEE (1.0 mg/mL) for 12 h in advance, and H_2O_2 (1 mM) was added for another 2 h. After the challenge, cells were collected ($1\sim5\times10^5$) with being washed twice by PBS, and then the binding buffer (500μL) was added to suspend the cells. Collected cells were labeled with Annexin V-APC (5 μL) and propidium iodide (PI) for 15 min at 25°C in dark. Finally, the apoptosis condition of cells was detected by flow cytometry (FACS AriaIIu, BD Bioscience, USA) using the Diva Cytometer software (BD Bioscience, USA).

Following oxidative stress treatment, the four groups of cells were washed twice with PBS and then suspended in PBS containing 1mM EDTA. The suspended cells were ultrasonically treated on ice for 5min (1s working, 2s interval, 200 W) and centrifuged at 6,000 g at 4°C for 15 min. The supernatant was saved at -80°C for further use. In each plate, cells with medium alone were regarded as a negative control, cells with H_2O_2 (1 mM) were regarded as a positive control, and GSH was used for comparison. The protein concentration was measured by the BCA protein assay (Sigma Aldrich, Shanghai, China). Antioxidant enzyme activity including glutathione reductase (GR), catalase (CAT), and glutathione peroxidase (GPx) was determined using a kit from Jiancheng (Nanning, China).

2.5. Statistical analysis

Conventional cell-based experimental results were expressed as the mean ± SD value (n=3). Statistical analyses were performed using SAS software (version 9.0). The statistical significance was evaluated using one-way ANOVA followed by Duncan's multiple-range test. *P* values less than 0.05 were considered significant.

3. Results and discussion

3.1. Working process of cell-based biosensor

Generally speaking, the detection of H_2O_2 by biosensor was well known and the fabrication of modified technique was also widely used to promote the sensitivity of electrodes. However, few studies have focused on the usage of biosensor on the detection of antioxidant effect of sample based on the ROS generation in cells. Following with the previous research, we produced the idea that the detection of H_2O_2 could reflect the ROS level, which would also be cited to indicate the antioxidant capacity based on the cell cultivation with antioxidant peptides in advance (Ge et al., 2018). Thus, we try to fabricate a cell-based biosensor following the procedure in the Scheme 1. The first step was to construct the electrode with platinum particle and then drop the Ag NWs on its surface. The second step was to prepare the hydrogels by GO, NaAlg, and DMEM. Then the cell suspension was added to mix with hydrogels together, during which the cells could keep the active inside. Then, the cell hydrogels were dropped on the working platform with stabilization so as to keep the cell active and stable on the surface of electrode. Finally, the cell-based biosensor was connected with the electrochemical workstation for the detecting of H_2O_2 levels.

When the cells were stimulated by H_2O_2, oxidative stress would generate with a series of radical chain reaction and then be following with damage on the membrane and the internal cell structures (Wang et al., 2015). Once treated with an antioxidant in advance, the H_2O_2 levels could be reduced by resisting continuous oxidative

stimulation with the cytoprotective effect to enhance the enzyme activity in the cell (Shi et al., 2014b). Hence, the antioxidant capacity could also be determined by evaluating H_2O_2 level in cell.

Known from the previous study, the Ag NWs could promote the reduction of H_2O_2 and also reduce the potential voltage energy in a redox reaction (Yang et al. 2012). In the working system, $Fe(CN)_6^{3-/4-}$ (1.0 mM) was the conductive solution, and H_2O_2 was added or generated in the working solution. As differential potential pressure was needed to promote redox reactions, there were two peak currents in the cell-based biosensors that can be explained by the following reaction:

Peak I $\quad Fe^{3+} + e^{-} \rightarrow Fe^{2+}$ (Reduction)

Peak Ⅱ $\quad H_2O_2 + 2\,H^{+} + 2e^{-} \rightarrow 2\,H_2O$ (Reduction)

3.2. Characterization of Pt NPs and Ag NWs

The morphology of Pt NPs was examined by SEM as shown in Fig. 1A. Bright spots were randomly distributed along with the bare gold electrode, indicating that the Pt NPs have successfully electroplated similarly to the findings of Bai et al. (2016). From the SEM image, the diameter of Pt NPs was mainly in the range of 200 nm to 500 nm. Although the Pt NPs did not show uniform shape or size, they were distributed throughout the surface of the bare electrode, and thus could be considered as nanoparticle ensembles (Chakraborty and Raj, 2009). The shape and size of nanostructured silver were important for the catalytic action in the surface plasmon response. Studies have reported that a diameter of 200 nm was suitable for the detection of H_2O_2 (Xia et al., 2015). From the image in Fig. 1B, the diameter of Ag NWs was approximately 200 nm which were linearly arranged contributing to the electrochemical catalysis in working system. In addition, the XRD pattern of silver nanowires is shown in Fig. 1C. The four sharp diffraction peaks of silver nanowires

(2θ=38.00°, 44.20°, 64.30° and 77.34°) were obvious and could be compiled with reflection lines of (111), (200), (220) and (311), respectively (Xia et al., 2015). The face-centered cubic crystal of silver was reflected in the calculated lattice constant of 4.0857Å, which was closely associated with the previous report of synthesized silver wires. The ratio intensity of peak (111) and (200) was 5.03, which was much higher than the theoretical value of 2.5 with the implied character of peak (111) crystalline planes being significantly enriched in the silver nanowires (Liu and Hu, 2009).

Ag NWs possess excellent catalytic activity for the reduction of H_2O_2. The concentration of Ag NWs could also alter the surface area of electrodes and change the conductivity of biosensor (Li et al., 2014). In a previous study, the dielectric constant was affected by concentration of Ag NWs and the most sensitive nanofiber webs contained 1.5 wt% Ag NWs in the poly solution (Kalaitzidou et al., 2008). In order to fabricate a highly sensitive biosensor, a gradient concentration of Ag NWs was dropped on the Pt NPs/GE to evaluate the optimum concentration for modified electrode. The sensitivity of Pt NPs/GE increased and then diminished under 0.16~20 mg/mL as shown in supplementary Fig. S1. The peak current in DPV increased within the concentration of 0.16~2.5 mg/mL and then decreased gradually within 2.5~20 mg/mL. The peak current value was 98.22 μA at 2.5 mg/mL, which shown to be the optimum concentration for the sensitivity of biosensor.

3.3. Characteristics of cell-based biosensors

The application of Pt NPs/Ag NWs/GE biosensors was explored to detect the sensitivity by CV, DPV and EIS in $Fe(CN)_6^{3-/4-}$ (1.0 mM) solution. As shown in Fig. 2A, the CV of bare gold, Pt NPs/ GE, Pt NPs/Ag NWs/GE and NaAlg/GO/ Pt NPs/Ag NWs/GE all yielded a typical redox peak with current peak values of 98.9 μA, 118.3 μA, 129.4 μA, and 70.1 μA, respectively (Fig. 2B). Pt NPs/Ag NWs/GE had a

relatively higher current peak than Pt NPs/ GE and bare gold, indicating that the two steps for the fabrication of electrode possess a good electric conducting property and is more sensitive than the bare gold electrode. The same tendency could also be known from the detection of H_2O_2 by modified electrode in steps as shown in the Fig. S2. When covered by hydrogels of NaAlg/GO as shown in line④in Fig. 2B, the current decreased simultaneously as the increased charge transfer resistance in $Fe(CN)_6^{3-/4-}$ on the surface of electrode implying the weak conductivity compared with that of the Pt NPs/Ag NWs/GE. In another way, it also successfully indicated that the hydrogels of NaAlg/GO could be stale on the working platform.

Following with the Randles-Sevcik equation, the concentration was the most important factor to peak current among all the influencing factors with the curtained electrochemical measurement system (Welch et al., 2005). To select a suitable cell concentration, the EIS of a gradient cell from 1×10^3~1×10^8 cells/mL were encapsulated inside the NaAlg/GO hydrogels so as to keep the excellent property of biosensor (Fig. 2C, curve d to i). The R_{et} values were simulated and then reflected by EIS pattern which was shown to be enhanced with the increase of cell concentration. However, the impedance of modified electrode was steady above cell concentration of 1×10^6 cells/mL in Fig. 2D. Based on the R_{et} values, a linear relationship was found at cell concentrations of 10^3~10^6 cells/mL with the correlation index of 0.988 which was in accordance with the study of Ge et al. (2018). There were no significant differences under the 10^6, 10^7 and 10^8 cells/mL with the R_{et} value of 1279.67 Ω,1314.43 Ω and 1333.49 Ω, respectively (P>0.05). Compared with the stable impedance of modified electrodes at different cell concentrations, 10^6 cells/mL was chosen for further experiments to determine the antioxidant capacity of DLEE using the cell biosensor.

After being detected with a gradient concentration of H_2O_2 (0.2~1000 μM), two peak currents appeared with the second peak being much larger than the first one (in the supplementary of Fig.S3). Compared with the CV and DPV of Pt NPs/Ag NWs/GE, the second peak appeared only after the addition of H_2O_2 to the working system, demonstrating that the second peak was the signal of H_2O_2. With increased H_2O_2, the second current peak value was increased incrementally. In order to keep the uniform distribution of H_2O_2 in the working solution, the magnetic stirrers were used and the curve DPV was shown to be undulated in Fig.3A. Oxidative peaks were enhanced gradually with the increase of H_2O_2 and the peak appeared at -0.1 V. A linear range from 0.2~2 μM was shown in the Fig. 3B with the RSD < 5% in every point of concentration. The linear equation was calculated as *Ip* (μA) =27.009 C + 3.1523 with a correlation coefficient of 0.991. The limit of detection (LOD) was counted as LOD=3 s/m. Here, s represents the standard deviation of blank sample, and m represents the slope of standard lines. From the review of the previous study, the detection line of biosensor fabricated by Ag NWs or Pt NPs would also vary when they were modified on the different electrode materials like glassy-carbon, platinum, gold, and anodic aluminum oxide as shown on the Table S1. In the current study, the detection limit of Pt NPs/Ag NWs/GE was 0.12 μA and the sensitivity was 27.01 μA/μM which was in a relatively high level. Based on the above tests, we conclude that Pt NPs/Ag NWs/GE is a relatively sensitive detector for the investigation of H_2O_2 and also simply operated on the fabrication of cell-based biosensor.

NaAlg/GO is widely used in the area of biomedical and chemical engineering with nontoxic, low-cost and high strength properties. The negative ions between NaAlg and GO cause electrostatic repulsions so as to generate a uniform spinning structure with the biological function keeping the cell active (He et al., 2012). The SEM image of

NaAlg/GO is shown in Fig. 3C with the obvious spinning structure. Caco-2 cells were embedded in the NaAlg/GO with the complete cell morphology as the chorionic villus was clearly observed (Fig. 3D). Once treated with the stimulation of H_2O_2, the cell membrane was destroyed and the chorionic villus surface also disappeared with some cavern generated in part (Fig. 3E). In addition, some fragments adhered to the membrane and cavern-like distribution implied that the intracellular oxidative stress could be evaluated by the external oxidation reduction signal. Thus, the oxidative level in Caco-2 could be investigated by CV and DPV pattern.

As the anti-interference ability was also a major challenge for biosensor, we chose ascorbic acid (AA), oxalic acid (OA), and glucose (GLU) as the interference of electrode with the DPV response (Xia et al., 2015). As shown in Fig.S4., the peak value of H_2O_2 was 76.05 μA with the detection by Ag NWs/Pt NPs/GE electrode. With the interference of AA, OA, and GLU at the same concentration of H_2O_2, there were no significant differences with the peak value of H_2O_2 (P>0.05). The results showed that there were negligible responses to current values after the injection of AA, OA and GLU, which indicated that the biosensor could keep stable with the detection of H_2O_2. In addition, a relative standard deviation (R.S.D) of 6 % with 6 parallel measurements showed an acceptable reproducibility. Even after 15 days storage at room temperature, the current response of modified electrode was 85% of the original values. The above results indicating that the Pt NPs/Ag NWs/GE biosensor showed remarkable stability and reproducibility, which is suitable for the evaluation of antioxidant effect of sample.

3.4. Cell-based measurement of antioxidant activity

The purification and identification of antioxidant peptide DLEE from dry-cured Xuanwei ham were published in our previous study (Xing et al., 2016). The chemical

assay was operated by scavenging free radicals as well as the evaluation of total antioxidant capacity (T-AOC) in Table.S2. DLEE showed scavenging capacity on $ABTS^+$ similar to GSH. The superoxide, the DPPH radical scavenging effect and the ORAC value were slightly lower than GSH. Furthermore, there were no significant differences between synthetic and purified DLEE in T-AOC value (P>0.05). We further investigated the cytoprotective effects of DLEE in Caco-2 cells using the cell-based biosensor to evaluate the capacity of inhibiting oxidative stress on the Caco-2 cells. Prior to the fabrication of NaAlg/GO hydrogels, four groups of 1×10^6 Caco-2 cells were collected and dissolved in DMEM. The antioxidant capacity of DLEE and GSH as determined by DPV analysis is shown in Fig. 4A. The peak current of blank group was 50.03 μA. The peak values for DLEE and GSH treatment ranged from 53.53~63.77 μA and 52.78~62.09 μA respectively at the concentrations of 0.5, 1.0 and 1.5 mg/mL.

The relationship between peak current values and the antioxidant capacity was reflected by RAC values as shown in Fig.4B. Antioxidant capacity increased gradually with increasing DLEE concentration. At the concentration of 0.5, 1.0 and 1.5 mg/mL, the RAC values for DLEE were 40.90%, 70.57% and 88.17%, and for GSH were 59.80%, 76.35% and 90.83%, respectively. There were significant differences in the antioxidant activity between DLEE and GSH at the same concentration which was consistent with the chemical assays. DLEE showed enhanced ability to inhibit the H_2O_2 level with increased concentration which supplied the basis for its functional effect on the protection of oxidative stress in cells. To confirm the results of the electrochemical methods, ROS generation in Caco-2 cells was detected under different treatments of DLEE and GSH. The results are depicted in Fig. 5A for fluorescence intensity with the treatments of 0.5, 1.0 and 1.5 mg/mL DLEE and GSH to protect against H_2O_2

stimulation. There was no added H_2O_2 in the control group and ROS were generated by cellular metabolism itself. The baseline value was 301, and fluorescence increased to 582 after H_2O_2 induction (P<0.05), indicating that H_2O_2 would cause the stimulation on cells and then give rise to the accumulation of ROS. When incubated with GSH or DLEE in advance, the fluorescence decreased gradually for the 0.5, 1.0, and 1.5 mg/mL groups. There were no significant differences between the 1.5 mg/ml DLEE and the H_2O_2 group (P>0.05). The fluorescence values decreased to 547 and 539 in the 1.0 mg/mL and 1.5 mg/mL of DLEE treatments, respectively, which were lower than that in H_2O_2 group. ROS levels in cells can also be observed visually in the fluorescence image in Fig. 5B. Compared with untreated cells (a), the H_2O_2-induced cell (b) showed more fluorescent spots in the field of view. In the DLEE group treated for 12 h in advance (c), these spots decreased similarly to the GSH group (d).

As was the important member of ROS molecules, H_2O_2 could mediate the oxidative damage on the membrane, DNA, and mitochondria in cells, leading to the apoptosis and necrosis event consequently (Zhang et al., 2015). Small changes in ROS in the intracellular space can play large roles in the early steps of apoptosis in Caco-2 cells. In the previous study on the antioxidant from grape seeds, the cell apoptosis tendency could be reduced with an early treatment (Dinicola et al. 2013). Based on the above facts, the generation of apoptosis in the cell could be related with the ROS level indirectly. In the current study, apoptosis was tested using the Annexin V-APC/PI Apoptosis Detection Kit by flow cytometry (Fig. 5C, Fig. 5D). The percentage of living cells decreased under H_2O_2 treatment (81.4%), while the early apoptosis in the DLEE (83.7%) and GSH (85.3%) treatments could be reduced to the levels of control. There were no significant differences for late-stage apoptosis or necrosis for the DLEE or GSH treatments compared with H_2O_2 treatment group (P>0.05). Therefore, from the

view of oxidative stress, DLEE could decrease the generation of ROS in cells and then inhibit the apoptosis in early stage. In coincide with the *vitro* oxidative stress experiment, the activities of antioxidant enzymes in Caco-2 cell were also shown in supplementary information with Table.S3. The CAT, GR and GPx are the main enzymes which could inhibit the generation of H_2O_2 in organisms. Compared with the incubation of GSH, a higher concentration of DLEE showed similar cytoprotective effects by enhancing the activity of GPx, GR and CAT. Therefore the conventional cell-based assays for antioxidant testing of DLEE implied the same tendency with the results of the electrochemical biosensor. Our work supplies the new methods for the evaluation of antioxidant peptides with a whole perspective from the free radicals scavenging activity, the endocellular oxidative stress level, the growth situation of cells to the H_2O_2 level in cells. Based on the results, the H_2O_2 level in Caco-2 cell could be decreased by the cultivation of bioactive peptide *DLEE* in advance.

4. Conclusion

In summary, we fabricated a cell-based biosensor by immobilizing living Caco-2 cells on Pt NPs/Ag NWs/GE to evaluate the antioxidant capacity of DLEE extracted from dry-cured Xuanwei ham. Based on the excellent catalytic characteristics of Ag NWs and Ag NWs, a novel biosensor was developed for the rapid detection of H_2O_2 with a LOD of 0.12 μA. The Caco-2 cells were stabilized in NaAlg/GO hydrogels with active cell activity for the fabrication of biosensor. Based on the peak current of DPV, the antioxidant capacity of DLEE could be calculated using the RAC equation and the RAC values indicated that DLEE had better antioxidant properties of 88.17% with the concentration of 1.5 mg/mL. In addition, ROS generation and apoptosis levels were also evaluated in coordination with electrochemical testing. The fluorescence intensity

and percentage of early apoptosis suggested that the treatment with DLEE could inhibit the generation of ROS in cells and decrease early apoptosis. Furthermore, DLEE appeared to have a protective effect on cellular defense to oxidative stress similar to that of GSH.

This method is developed to exploit a new technology for evaluating antioxidant properties based on measuring intercellular H_2O_2 levels. The proposed cell-based electrochemical method has substantial advantages over conventional assays and can be used to accurately evaluate the antioxidant capacity of other polypeptides on cells. This rapid, simple and sensitive method for the convenient detection of H_2O_2 in living cells could be potentially used for investigating the antioxidant capacities of natural extracts including functional peptides.

Acknowledgments

This research was supported by the National Key Research and Development Program of China (2016YFD0400703), the National Natural Science Foundation of China (31571853 and 31601535), the Natural Science Foundation of Jiangsu Province (No. BK20160459), the Priority Academic Program Development of Jiangsu Higher Education Institutions (No. 16KJB550008) and 2017 graduate practice innovation plan of Yangzhou University (SJCX170631). The authors gratefully thank Food Science College of Yangzhou University for valuable help to operate the electrochemical workstation as well as analyze the data.

References

Artursson, P., Palm, K., Luthman, K., 2012. Advanced Drug Delivery Reviews 64, 280-289.

Bai, Z.H., Li, G.Y., Liang, J.T., Su, J., Zhang, Y., Chen, H.Z., Huang, Y., Sui, W.G., Zhao, Y. X., 2016.Biosensors & Bioelectronics 82.185-194.

Chakraborty, S., Raj, C.R., 2009. Biosensors & Bioelectronics 24(11), 3264-3268.

Chen, X.M., Lin, Z.J., Chen, D.J., Jia, T.T., Cai, Z.M., Wang, X.R., Chen, X., Chen, G.N., Oyama, M., 2010. Biosensors & Bioelectronics 25(7), 1803.

Dinicola, S., Mariggiò, M.A., Morabito, C., Guarnieri, S., Cucina, A., Pasqualato, A., D'Anselmi, F., Proietti, S., Coluccia, P., Bizzarri, M., 2013. British Journal of Nutrition 110(5), 797-809.

Feng, R., Zhang, Y., Ma, H., Wu, D., Fan, H., Wang, H., Li, H., Du, B., Wei, Q., 2013. Electrochimica Acta 97(5), 105-111.

Gao, S., Oh, Y.B., Park, B.M., Park, W.H., Kim, S.H., 2012. Peptides 36(2), 199-205.

Ge, Q., Ge, P., Jiang, D., Du, N., Chen, J., Yuan, L., Yu, H., Xu, X., Wu, M., Zhang, W., 2017. Biosensors & Bioelectronics 99, 555.

He, Y., Zhang, N., Gong, Q., Qiu, H., Wang, W., Liu, Y., Gao, J., 2012. Carbohydrate Polymers 88(3), 1100-1108.

Jiang, D., Feng, D., Jiang, H., Yuan, L., Yongqi, Y., Xu, X., Fang, W., 2017.Biosensors & Bioelectronics 90, 436-442.

Kalaitzidou, K., Fukushima, H., Askeland, P., Drzal, L.T., 2008. Journal of Materials Science 43(8), 2895-2907.

Kim, J., Choi, K.S., Kim, Y., Lim, K.T., Seonwoo, H., Park, Y., Kim, D.H., Choung, P.H., Cho, C.S., Kim, S.Y., 2013. Journal of Biomedical Materials Research Part A 101(12), 3520–3530.

Lei, K.F., Wu, M.H., Hsu, C.W., Chen, Y.D., 2014. Biosensors & Bioelectronics 51(2), 16-21.

Li, B., Xu, C., Zheng, J., Xu, C., 2014. Sensitivity of pressure sensors enhanced by doping silver nanowires. Sensors 14(6), 9889.

Liu, C.Y., Hu, J.M., 2009. Biosensors & Bioelectronics 24(7), 2149-2154.

Liu, J., Bo, X., Zhao, Z., Guo, L., 2015. Biosensors & Bioelectronics 74, 71-77.

Liu, R., Xing, L., Fu, Q., Zhou, G.H., Zhang, W.G., 2016. Antioxidants 5(3).

Nandini, S., Nalini, S., Niranjana, P., Melo, J.S., Suresh, G.S., 2017. Sensors & Actuators B Chemical 245, 726-740.

Pillai, K., Costello, B., Oresajo, C., Ceccoli, J., 2006. US.

Prakash, P., Agarwal, R., Singh, N., Chauhan, R.P., Agrawal, V.V., Biradar, A.M., 2015. Sensor Letters 13(3), 219-222(214).

Samaraweera, H., Zhang, W.g., Lee, E.J., Ahn, D.U., 2011. Journal of Food Science 76(7), R143-R150.

Sarmadi, B.H., Ismail, A., 2010. Peptides 31(10), 1949-1956.

Shi, Y., Kovacs-Nolan, J., Jiang, B., Rong, T., Mine, Y., 2014a. Journal of Functional Foods 10(3), 35-45.

Shi, Y., Kovacs-Nolan, J., Jiang, B., Rong, T., Mine, Y., 2014b. Journal of Functional Foods 11(50), 571-580.

Sila, A., Bougatef, A., 2016. Journal of Functional Foods 21, 10-26.

Sudhakar, S., Nazeer, R.A., 2015. Journal of Functional Foods 14, 502-512.

Sun, M., Sheng, X., Hu, Y., 2006. Chinese Pharmaceutical Journal-Beijing 41(18), 1431.

Torres-Fuentes, C., Contreras, M.D.M., Recio, I., Alaiz, M., Vioque, J., 2015. Food Chem 180, 194-202.

Wang, L., Ding, L., Yu, Z., Zhang, T., Ma, S., Liu, J., 2016. Food Research International 90, 33-41.

Wang, S.L., He, L.J., He, T.B., Han, W., Wang, Q., 2015. Journal of Experimental Hematology 23(2), 552-556.

Welch, C.M., Banks, C.E., Simm, A.O., Compton, R.G., 2005. Analytical & Bioanalytical Chemistry 382(1), 12-21.

Xia, Q., Wang, H., Miao, Z., Li, J., Qiang, C., 2015. Talanta 139, 56.

Xing, L.J., Hu, Y.Y., Hu, H.Y., Ge, Q.F., Zhou, G.H., Zhang, W.G.,2016. Food Chem 194, 951-958.

Yang, X., Bai, J., Wang, Y., Jiang, X., He, X., 2012. Analyst 137(18), 4362-4367.

Zhang, D., Ren, L., Chen, G.Q., Zhang, J., Reed, B.M., Shen, X.H., 2015. Plant Cell Reports 34(9), 1499-1513.

Zhou, Y., Ma, Z., 2017. Sensors & Actuators B Chemical 249.

Figures

Scheme 1.The working process for the detection of H_2O_2 in Caco-2 cell-based Pt NPs/Ag NWs/GE biosensor.

Fig.1.(A) The SEM image of Pt NPs on the bare gold electrode.

(B) The SEM image and (C) XRD pattern of Ag NWs with the concentration of 2.5 mg/mL.

Fig.2. (A) Cyclic voltammograms and (B) Differential pulse voltammetry of biosensor electrode with ① Pt NPs/Ag NWs/GE, ② Pt NPs/GE, ③ bare GE, ④ NaAlg/GO/Pt NPs/Ag NWs/GE.

(C) Nyquist diagrams of (a) Pt NPs/Ag NWS/GE, (b) bare GE, (c) NaAlg/GO/Pt NPs/Ag NWs/GE, (d) to (i): 1×10^3 to 1×10^8 cells/mL of Caco-2 cells immobilized on NaAlg/GO/Pt NPs/Ag NWs/GE.

(D) Linear regression curve between cell concentrations and R_{et} value.

Fig.3.(A) DPV responses of the Pt NPs/Ag NWs/GE for the detection of H_2O_2 level in Caco-2 cells (from 0.2 to 1000 μM).

(B) The corresponding calibration plots between the peak currents and H_2O_2 concentrations (from 0.2 μM to 2 μM). The morphology of (C) NaAlg/GO, (D) Caco-2 cells and (E) Caco-2 cells treated with H_2O_2.

Fig.4. (A) The DPV of the Caco-2 cell-based sensor detected with DLEE and GSH, ①: H_2O_2 treated without peptides; ②④⑥: H_2O_2 treated with DLEE (0.5,1.0,1.5 mg/mL); ③⑤⑦: H_2O_2treated with GSH (0.5,1.0,1.5 mg/mL); ⑧: without any treatment as control group.

(B) The relative antioxidant capacity of DLEE and GSH.

Fig. 5.(A) The fluorescence intensity of ROS in Caco-2 cells incubated with DLEE and GSH. The control group represents the cells without H_2O_2 stimulation and H_2O_2 group represents the cells treated with H_2O_2 stimulation for additional 2 h.

(B) The fluorescence image of Caco-2 cells with different treatment.

(C) FACS analysis of apoptosis in Caco-2 cells with different treatment.

(D) The distribution of apoptosis in the different stage of Caco-2 cells.

(B, D) a represents control group; b represents the H_2O_2 treated group; c and d represent the DLEE and GSH (1.0 mg/mL) treated before the same H_2O_2 stimulation.

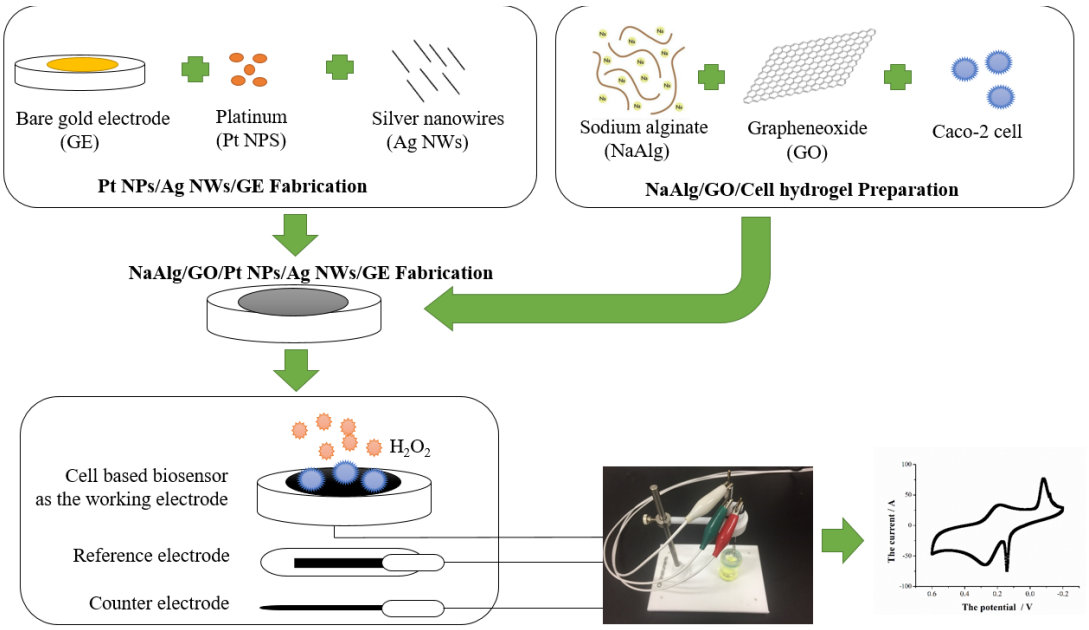

Scheme 1.The working process for the detection of H_2O_2 in Caco-2 cell-based Pt NPs/Ag NWs/GE biosensor.

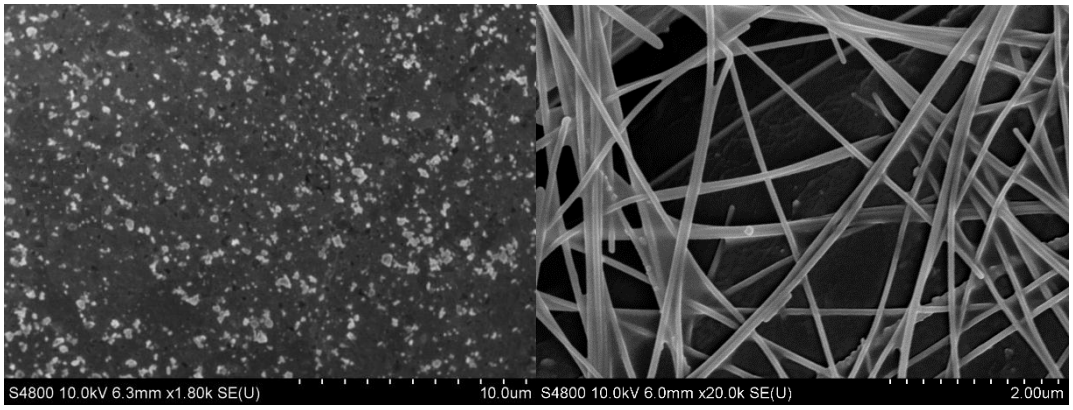

(A) (B)

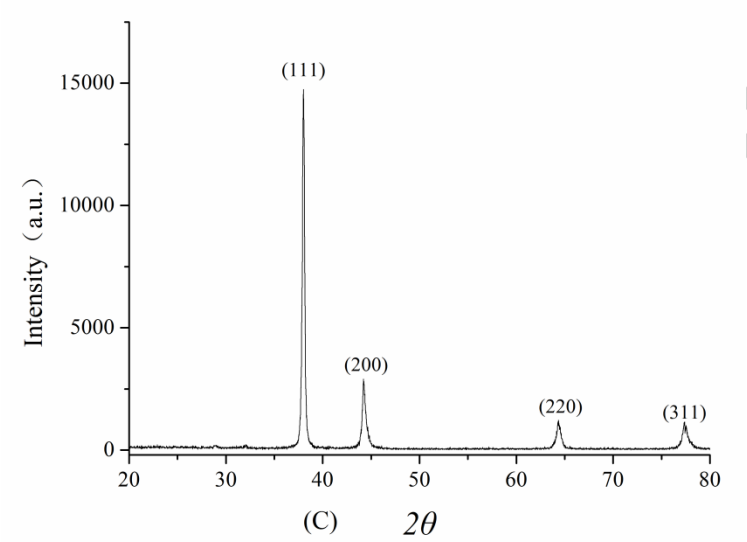

(C)

Fig.1. (A) The SEM image of Pt NPs on the bare gold electrode.
(B) The SEM image and (C) XRD pattern of Ag NWs with the concentration of 2.5 mg/mL.

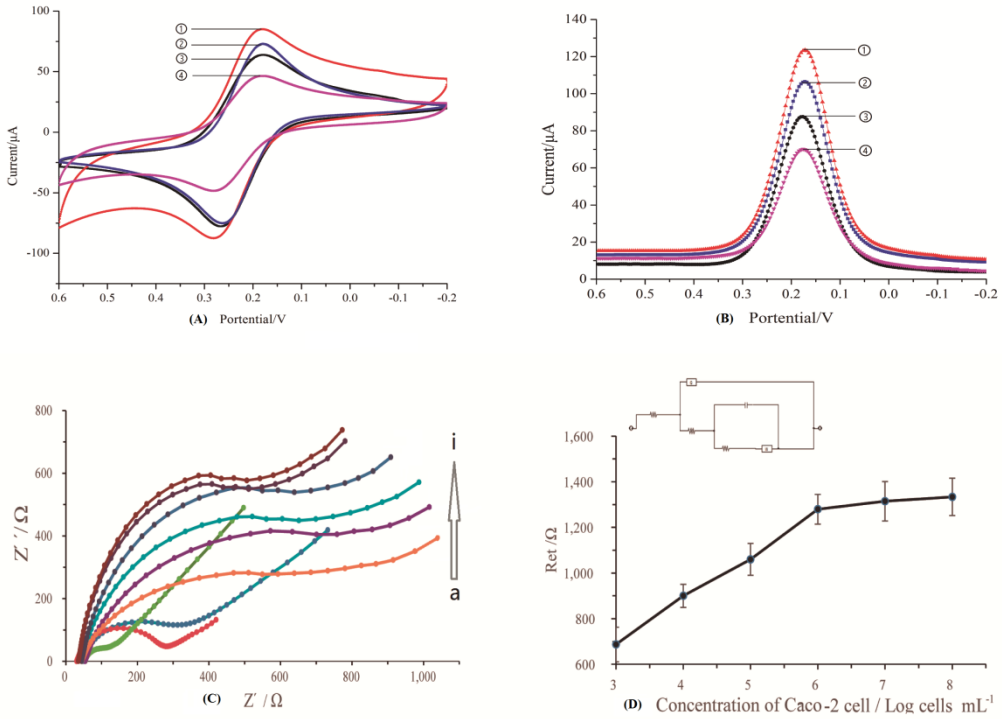

Fig.2. (A) Cyclic voltammograms and (B) Differential pulse voltammetry of biosensor electrode with ① Pt NPs/Ag NWs/GE, ② Pt NPs/GE, ③ bare GE, ④ NaAlg/GO/Pt NPs/Ag NWs/GE.

(C) Nyquist diagrams of (a) Pt NPs/Ag NWS/GE, (b) bare GE, (c) NaAlg/GO/Pt NPs/Ag NWs/GE, (d) to (i): 1×10^{3} to 1×10^{8} cells/mL of Caco-2 cells immobilized on NaAlg/GO/Pt NPs/Ag NWs/GE.

(D) Linear regression curve between cell concentrations and R_{et} value.

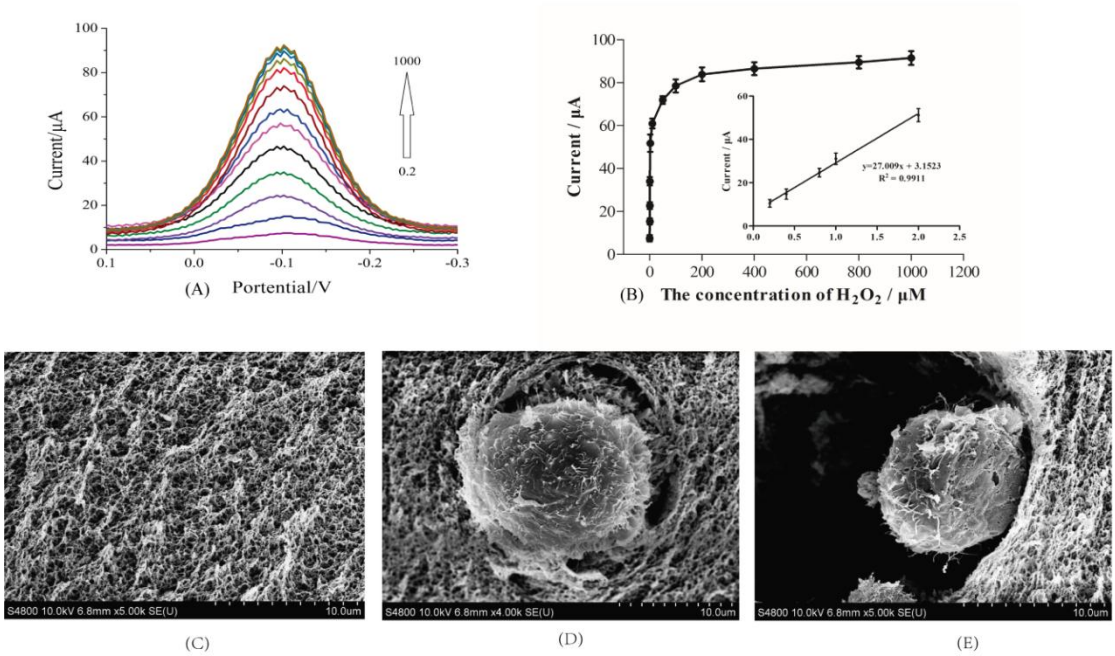

Fig.3. (A) The DPV responses of the Pt NPs/Ag NWs/GE for the detection of H_2O_2 (from 0.2 to 1000 μM). (B) The corresponding calibration plots between the peak currents and H_2O_2 concentrations (from 0.2 μM to 2 μM). The morphology of (C) NaAlg/GO, (D) Caco-2 cells and (E) Caco-2 cells treated with H_2O_2.

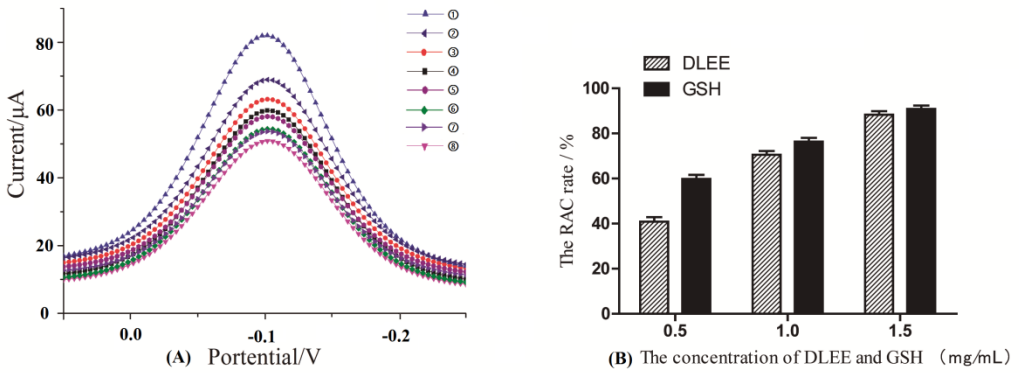

Fig.4.(A) The DPV of the Caco-2 cell-based senor detected with DLEE and GSH, ①: H_2O_2 treated without peptides; ②④⑥: H_2O_2 treated with DLEE (0.5,1.0,1.5 mg/mL); ③⑤⑦: H_2O_2 treated with GSH (0.5,1.0,1.5 mg/mL); ⑧ without any treatment as control group.

(B) Relative antioxidant capacity of DLEE and GSH (n=3).

(A) (B)

(D)

(C) (D)

Fig. 5. (A) The fluorescence intensity of ROS in Caco-2 cells incubated with DLEE and GSH. The control group represents the cells without H_2O_2 stimulation and H_2O_2 group represents the cells treated with H_2O_2 stimulation for additional 2 h.

(B) The fluorescence image of Caco-2 cells with different treatment.

(C) FACS analysis of apoptosis in Caco-2 cells with different treatment.

(D) The distribution of apoptosis in the different stage of Caco-2 cells.

(B, D) *a* represents control group; *b* represents the H_2O_2 treated group; *c* and *d* represent the DLEE and GSH (1.0 mg/mL) treated before the same H_2O_2 stimulation.

Highlights

- A platinized gold electrode plated with silver nanowires (Pt NPs/Ag NWs/GE) was fabricated to detect H_2O_2 redox signaling.
- Caco-2 cell sensors with 3D structure were established for antioxidant capacity evaluation.
- The antioxidant capacity of DLEE was assessed based on electrochemical detection of H_2O_2.